ISBN: 978-3-95450-214-1 ISSN: 2673-5490 doi:10.18429/JACoW-IPAC2021-WEPAB006

EIC CRAB CAVITY MULTIPOLE ANALYSIS*

Q. Wu†, Y. Luo, B. Xiao, Brookhaven National Laboratory, Upton, NY, USA
S. U. De Silva, Old Dominion University, Norfolk, VA, USA
J. A. Mitchell, CERN, Geneva, Switzerland

Abstract

Crab cavities are specialized RF devices designed for colliders targeting high luminosities. It is a straightforward solution to retrieve head-on collisions when crossing angle existing in the design in order to fast separate both beams after collision. The Electron Ion Collider (EIC) has a crossing angle of 25 mrad, and will use local crabbing to minimize the dynamic aperture requirement throughout the rest of the ring sections outside the interaction region. The current crab cavity design for the EIC lacks axial symmetry. Therefore, their higher order components of the fundamental deflecting mode have a potential of affecting the long-term beam stability. We present here the multipole analysis and preliminary particle tracking results from the current crab cavity design.

INTRODUCTION

In the latest Electron Ion Collider (EIC) design [1], a single interaction region occupies a ±100 m region with the detector in the center at the six o'clock location in the current Relativistic Heavy Ion Collider (RHIC) tunnel. To avoid unwanted interactions, a large full crossing angle of 25 mrad is required to quickly separate the two beams after collision. Local crabbing scheme is adopted in the EIC design to recover the luminosity loss due to the crossing angle. A set of crab cavities with frequencies of 197 MHz and 394 MHz will be installed on each side of the detector. The crab cavity locations are chosen such that the phase advance between the two sets of the cavities are 180 degree, and the detector in the center is 90 degree apart from each set. The interaction region layout is shown in Fig. 1, and also described in [2].

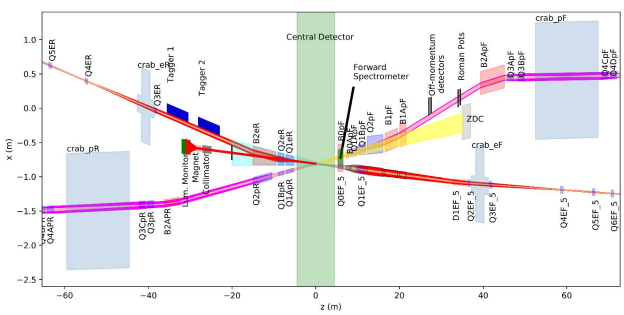

Figure 1: Current interaction design of EIC. The light blue boxes indicate location of crab cavities for both rings.

To relax the cavity design with the required voltage, the beta function at the crab cavities is lifted to 1300 m. With such configuration, these cavities may contribute some limitation to the dynamic aperture of the interaction region with their multipoles of the crabbing mode. Analysis of crab cavities for Large Hadron Collider with similar design have been analyzed in other references [3]. Calculation of the multipole strength with the crab cavity [4] design is carried out with the CST Suite [5] and a python code [6], and the dynamic aperture is calculated in SimTrack [7] with preliminary results.

MULTIPOLE ANALYSIS

Given the axial asymmetry in RF cavity designs, the fundamental mode electric field can be expanded into a series of multipoles in a similar fashion as is done for static field magnets. Different from the magnets, in the crab cavity, all multipoles are in phase with the main deflecting mode.

The multipoles of the crab cavity can be expressed from the Panofsky–Wenzel (PW) theorem. Assuming the particle with speed c does not change trajectory inside the cavity $[0, L]$, the longitudinal momentum change inside cavity gives:

$$\Delta p_{\parallel} = e^{i\omega z/c+\psi}\left(\frac{q}{c}\int_0^L E_s\,(r,\theta,s)\,e^{i\omega s/c}ds\right).$$

From PW theorem,

$$\nabla\,(\Delta p) = 0$$

$$\frac{\partial}{\partial z}\,(\Delta p_{\perp}) = -\nabla_{\perp}\,(\Delta p_{\parallel}).$$

Therefore

$$\Delta p_{\perp} = e^{i\omega z/c+\psi}\left(\frac{iq}{\omega}\nabla_{\perp}\int_0^L E_s\,(r,\theta,s)\,e^{i\omega s/c}ds\right).$$

Expand the integral inside the parentheses in Fourier series:

$$\begin{aligned} A(r,\theta) &= \frac{iq}{\omega}\int_0^L E_s\,(r,\theta,s)\,e^{i\omega s/c}ds \\ &= \sum_{n=1}^{\infty}\frac{r^n}{n}\,(b_n\cos n\theta + a_n\sin n\theta). \end{aligned}$$

Then the strength of the multipoles, which are the coefficients in the equation above can be expressed as:

$$b_n = \frac{1}{\pi}\int_0^{2\pi}\frac{n}{r^n}A(r,\theta)\cos n\theta d\theta$$

$$a_n = \frac{1}{\pi}\int_0^{2\pi}\frac{n}{r^n}A(r,\theta)\sin n\theta d\theta.$$

Each a_n and b_n are the skew and normal multipole coefficient of the $2n^{th}$ pole respectively, with b_1 being the main crabbing dipole mode. Similarly, the momentum change is:

$$\Delta p_{\parallel} = -e^{i\omega z/c+\psi}\frac{i\omega}{c}A(r,\theta)$$

$$\Delta p_{\perp} = e^{i\omega z/c+\psi}\nabla_{\perp}A(r,\theta).$$

* Work supported by Brookhaven Science Associates, LLC under Contract No. DE-SC0012704 with the U.S. Department of Energy.
† qiowu@bnl.gov

ISBN: 978-3-95450-214-1 ISSN: 2673-5490 doi:10.18429/JACoW-IPAC2021-WEPAB006

MULTIPOLE CALCULATION AND CONVERGENCE STUDY

A vacuum volume model of the RF Dipole crab cavity design at 197 MHz for EIC is shown in Fig. 2. This model is used for the multipole convergence study and preliminary dynamic aperture tracking. The EM field for this design is shown in Fig. 3.

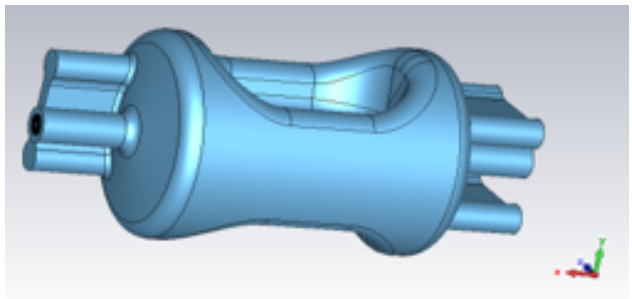

Figure 2: Vacuum volume of the EIC crab cavity.

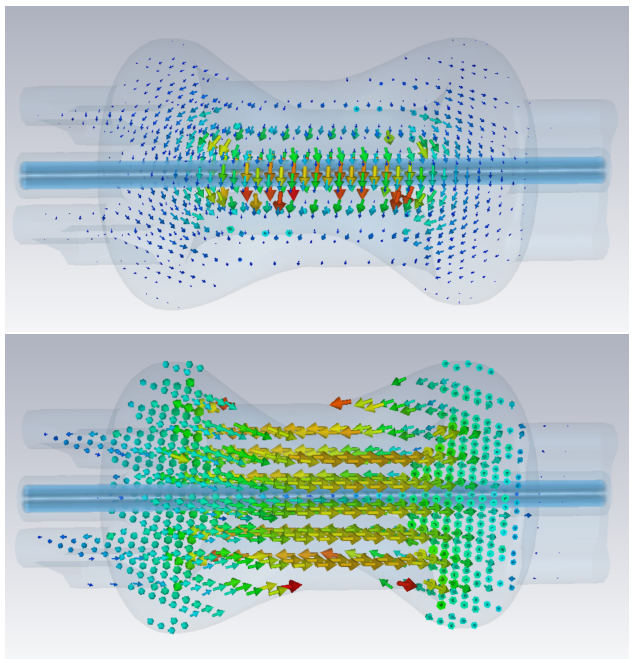

Figure 3: Electric (top) and Magnetic (bottom) field of the crab cavity.

The EM field at a specified radius r along the beam axis is extracted from the CST simulations, and then integrated in a Python code to calculate for the multipole strength at each order. The normal multipole strength b_n along the beam axis is calculated by local integration as shown in Fig. 4.

Two methods were used to calculate the multipoles: Using only the longitudinal electric field at radius r with Panofsky–Wenzel Theorem (PW), and using both transverse electric and magnetic field at the same radius to calculate the Lorentz Force (LF). The two methods converge differently with the mesh size and the radius r. Based on the symmetry of the model and the horizontal placement configuration,

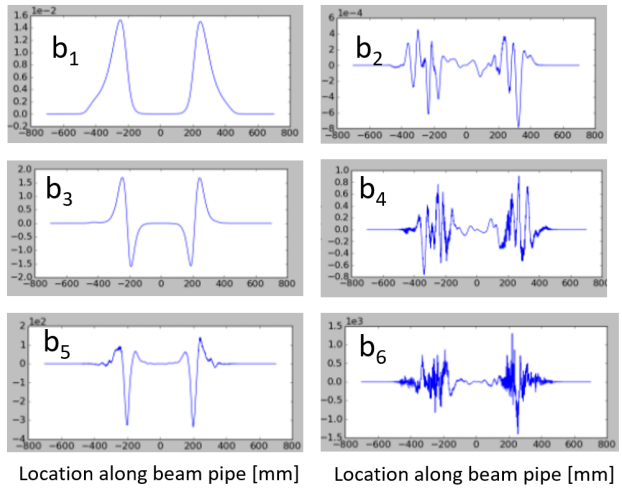

Figure 4: Normal multipole strength b_n along beam axis. The vertical axis of each plot has the unit of $\mathrm{mTm/m}^{n-1}$.

all skew multipole strength a_n should be negligible, compared to the normal multipole strength b_n. In addition, the quadrupolar component b_2, b_4, and b_6 are zero in the case of perfect symmetry. However, it is worth to notice that due to fabrication errors and ancillary components, these values should deviate from zero during operation. The tolerance of the fabrication and alignment errors should be defined with dynamic aperture tracking with crab cavity multipoles.

Higher order multipoles are harder to converge due to signal to systematic noise ratio in simulation (same problem in actual measurement), therefore the value of b_4 and b_6 are used in the multipole calculation to determine the parameters in EM field simulation for the cavity, as well as compare the two methods used for calculation. Figures 5 and 6 shows the comparison of PW and LF methods with different mesh size and radius r respectively. In both comparisons, LF method gives relatively closer to zero b_4 and b_6 with acceptable mesh size and radius.

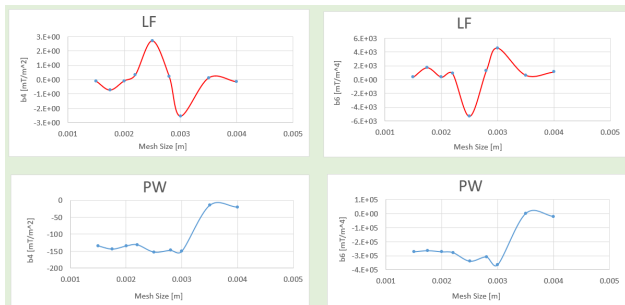

Figure 5: Comparison of PW and LF methods with respect to the mesh size in EM field simulation.

The b_n and a_n values used for dynamic aperture tracking are listed in Table 1, with 2 mm mesh size in both transverse and longitudinal directions in EM simulation and extracting the field at the radius of 20 mm.

ISBN: 978-3-95450-214-1 ISSN: 2673-5490 doi:10.18429/JACoW-IPAC2021-WEPAB006

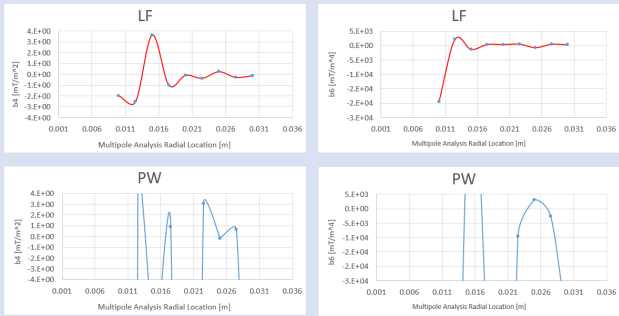

Figure 6: Comparison of PW and LF methods with respect to the specified field extraction radius in EM field simulation.

Table 1: Multipole Strength

n	b_n [mTm/m^{n-1}]
1	2.810×10^{1}
2	3.542×10^{-5}
3	4.412×10^{2}
4	-8.561×10^{-2}
5	-2.199×10^{4}
6	3.513×10^{2}

Dynamic Aperture Tracking

The dynamic aperture tracking included all components in the interaction region with errors on the magnets. Preliminary radial dynamic aperture tracking results are shown in Fig. 7.

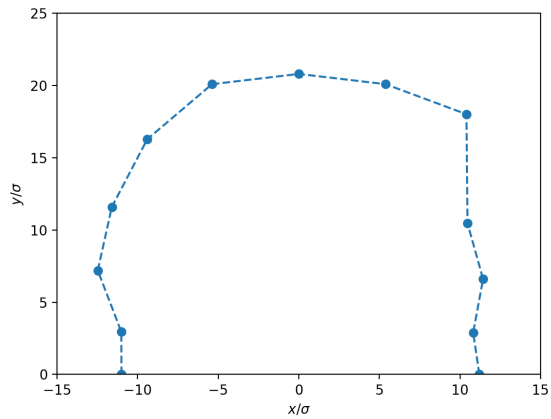

Figure 7: Preliminary tracking results of the DA tracking with crab cavities.

The dynamic aperture in Fig. 7 is defined as $N = \sqrt{(N_x^2 + N_y^2)}$, where N_x and N_y are the two orthogonal phase space for DA searching in the unit of rms beam size in x and y directions.

The tracking assumed a total operation voltage of 25.82 MV from each 197 MHz crab cavity set, and the 394 MHz cavities are not included here. The simulation also assumed all crab cavity multipoles located at the center of the cavity chain at the installation site. The skew multipole strength a_n is multi-orders of magnitude smaller compare to the strength of the normal multipoles, with the assumption of ideal cavities and precise alignment during installation. Therefore, these result shown in Fig. 7 neglected the affect from the skew multipoles.

CONCLUSION

In the current design, the EIC will install two sets of crab cavities on each side of the detector symmetrically to implement local crabbing. These cavities are not axial symmetric and therefore the excited higher order multipoles may provide some limitation to the dynamic aperture in the interaction region. The analysis of these multipoles provided guidance for parameters during EM field simulations with limited computing resources. The preliminary tracking results show that the dynamic aperture with crab cavities is 11 sigma of the radial beam size.

The next steps for multipole calculation would be include RF couplers and empirical fabrication error to the cavity EM field, as well as allow some tolerance for the installation of these cavities in the tunnel.

ACKNOWLEDGEMENT

The authors would like to thank Kai Papke for sharing the Macro for extracting the EM field from the CST Studio.

REFERENCES

[1] C. Montag *et al.*, "Design Status Update of the Electron-Ion Collider", presented at the 12th Int. Particle Accelerator Conf. (IPAC'21), Campinas, Brazil, May 2021, paper WEPAB005, this conference.

[2] H. Witte *et al.*, "The Interaction Region of the Electron-Ion Collider", presented at the 12th Int. Particle Accelerator Conf. (IPAC'21), Campinas, Brazil, May 2021, paper WEPAB002, this conference.

[3] J. B. García *et al.*, "Long Term Dynamics of the High Luminosity Large Hadron Collider with Crab Cavities", *Phys. Rev. Accel. Beams*, vol. 19, p. 101003, 2016. doi:10.1103/physrevaccelbeams.19.101003

[4] S. De Silva *et al.*, "Design of an RF-Dipole Crabbing Cavity System for the Electron-Ion Collider", presented at the 12th Int. Particle Accelerator Conf. (IPAC'21), Campinas, Brazil, May 2021, paper MOPAB393, this conference.

[5] CST Microwave Studio Suite 2020, https://www.3ds.com/products-services/simulia/products/cst-studio-suite/.

[6] J. A. Mitchell, "Higher Order Modes and Dampers for the LHC Double Quarter Wave Crab Cavity", Ph.D. thesis, Lancaster University, Lancaster, United Kingdom, 2019.

[7] Y. Luo, "SimTrack: A compact c++ code for particle orbit and spin tracking in accelerators", *Nucl. Instrum. and Methods A*, vol. 801, pp. 95-103, 2015. doi:10.1016/j.nima.2015.08.014